Nonlinear behavior of a reaction-diffusion system of the photochemistry within the mesopause region

G. Sonnemann[1] and A. M. Feigin[2]
[1]*Institute of Atmospheric Physics at the University of Rostock, D-18225 Kühlungsborn, Germany*
[2]*Institute of Applied Physics, Plasma Physics and High-Power Electronics Department, Russian Academy of Sciences, 603600 Nizhny Novgorod, Russia*
(Received 8 September 1998)

The photochemistry of the mesopause region entails a driven chemical oscillator enforced by solar shortwave irradiation. Zero-dimensional calculations show that this oscillator is able to produce nonlinear reactions like cascades of subharmonics or chaos. We investigate what will happen if this system is subjected to atmospheric diffusion. We discuss the system response and introduce different kinds of bifurcations. [S1063-651X(99)15202-4]

PACS number(s): 05.45.−a, 92.60.Hp, 82.40.Bj, 94.10.Lf

I. INTRODUCTION

Reaction-diffusion systems (RDSs) play a great role in nature. The pattern formation on the basis of RDSs may be mentioned. Here we investigate a special photochemical system of the mesopause region. The mesopause is the transition region between the mesosphere and thermosphere, and is located near 85 km according to the mean atmosphere model assumption. (In reality it can vary considerably if one uses the definition criterion: The mesopause is the height of the actual lowest temperature.) This height region is one of the most sensitive and least explored regions of the atmosphere. It divides that part of the atmosphere which is mainly influenced by solar variability—the thermosphere—from that one which is chiefly influenced by meterological processes—the mean and lower atmosphere including the mesosphere.

The lowest temperatures which can be observed anywhere in nature around the globe occur in summer in the mesopause region. That is why this region is thermically rather sensitive. Due to the recombination of atomic oxygen which is transported downward from the thermosphere, the chemical heating rate reaches maximum values within the mesopause region. Hence the investigation of the chemistry of the mesopause region is of great significance. The chemistry feeds back to the dynamics, and that influences the transport of chemically active minor constituents again.

The atmosphere is essentially vertically stratified. While the vertical scale, for example for the density change of the important chemical constituents, only amounts to some kilometers, the horizontal scales can be many hundreds or thousands of kilometers in magnitude. This fact justified the frequently used condition to consider the chemical composition of the atmosphere in one-dimensional models. The use of such models has the advantage that the height resolution can be made essentially finer, and the system integrated more accurately, than could be realized in multidimensional models. The interpretation of the results is easier, and they correspond to reality sufficiently well. Last but not least, this natural one dimensionality is an advantage for theoretical investigations in the field of chaos research.

II. BRIEF INTRODUCTION TO THE PHOTOCHEMISTRY OF THE MESOPAUSE REGION

The chemistry of the mesopause is, in a good approximation, a so-called odd oxygen–odd hydrogen chemistry. The oxygen constituents, which are characterized by an odd number of oxygen atoms (one or three), belong to the odd oxygen family. These are atomic oxygen O and ozone O_3. In an analogous way the hydrogen radicals H, OH, and HO_2 have been called odd hydrogens in contrast to H_2O, H_2, or CH_4, possessing an even number of hydrogen atoms. Both chemical families are in close interaction with one another. The odd hydrogen family destroys the odd oxygen family catalytically. The odd oxygen family changes the composition of the odd hydrogen family at the same time. The catalytic destruction takes place via two essential cycles:

$$O_3+H\rightarrow O_2+OH, \quad O_3+OH\rightarrow O_2+HO_2,$$

$$O+OH\rightarrow O_2+H, \quad O+HO_2\rightarrow O_2+OH,$$

$$\text{net:} \quad O_3+O\rightarrow 2O_2, \quad \text{net:} O_3+O\rightarrow 2O_2.$$

A third chain, but not so important in the mesopause region, is given by

$$O+OH\rightarrow O_2+H,$$

$$H+O_2+M\rightarrow HO_2+M,$$

$$O+HO_2\rightarrow O_2+OH,$$

$$\text{net:} \quad O+O\rightarrow O_2.$$

In addition to this, the odd oxygens are able to destroy themselves directly by the reactions

$$O+O_3\rightarrow 2O_2 \quad \text{and} \quad O+O+M\rightarrow O_2+M.$$

M means a chemically uninvolved collision particle which absorbs released energy and momentum. The loss of hydrogen radicals happens via reactions among one another, and they lead to the formation of even hydrogen molecules. The formation of odd components mainly takes place by photoly-

TABLE I. Most relevant reactions of the mesopheric chemistry.

Reaction	Rate constant[a]
(1) $O+O_3 \rightarrow 2O_2$	$(8.00\times10^{-12})\exp(-2060/T)$
(2) $O_3+H \rightarrow O_2+OH$	$(1.40\times10^{-10})\exp(-470/T)$
(3) $O+OH \rightarrow O_2+H$	$(2.20\times10^{-11})\exp(120/T)$
(4) $O_3+OH \rightarrow O_2+HO_2$	$(1.60\times10^{-12})\exp(-940/T)$
(5) $O+HO_2 \rightarrow O_2+OH$	$(3.00\times10^{-11})\exp(200/T)$
(6) $H+HO_2 \rightarrow O_2+H_2$	5.60×10^{-12}
(7) $H+HO_2 \rightarrow 2OH$	7.30×10^{-11}
(8) $OH+OH \rightarrow O+H_2O$	$(4.20\times10^{-12})\exp(-240/T)$
(9) $OH+HO_2 \rightarrow O_2+H_2O$	$(4.80\times10^{-11})\exp(250/T)$
(10) $HO_2+HO_2 \rightarrow O_2+H_2O_2$	$(2.30\times10^{-13})\exp(600/T)$
(11) $O+O_2+M \rightarrow O_3+M$	$(6.90\times10^{-34})(300/T)^{1.25}\alpha_1$
	$(+6.20\times10^{-34})(300/T)^{2}\alpha_2$
(12) $O+O+M \rightarrow O_2+M$	$(3.80\times10^{-30})\exp(-170/T)/T\alpha_1$
	$(+4.8\times10^{-33})(300/T)^{2}\alpha_2$
(13) $O+OH+M \rightarrow HO_2+M$	$(2.00\times10^{-32})\alpha_2$
(14) $O_2+H+M \rightarrow HO_2+M$	$(5.50\times10^{-32})(300/T)^{1.4}\alpha_2$
(15) $OH+H+M \rightarrow H_2O+M$	$(1.38\times10^{-24})/T^{2.6}\alpha_2$
(16) $O_2+h\nu \rightarrow 2O$	(3.15×10^{-8})(92 km)
(17) $H_2O+h\nu \rightarrow H+OH$	2.40×10^{-6}
(18) $O_3+h\nu \rightarrow O_2+O$	7.10×10^{-3}

[a]Photodissociation constants are in units of s^{-1}, two body rate constants in units of $cm^3\,s^{-1}$, and three body rate constants in units of $cm^6\,s^{-1}$. $\alpha_1=[O_2]/[M]$ and $\alpha_2=[N_2]/[M]$.

sis of O_2 and H_2O which forms atomic oxygen in $O_2+h\nu(\lambda\lesssim242\,\text{nm})\rightarrow 2O$, and the hydrogen radicals H and OH in $H_2O+h\nu(\lambda\lesssim240\,\text{nm})\rightarrow H+OH$. Atomic oxygen reacts with O_2 in a three body (third order) reaction forming ozone: $O+O_2+M\rightarrow O_3+M$. This is the only effective ozone formation process in the atmosphere. Ozone itself can be dissociated very easily into its initial products O and O_2, which form back ozone. For this reason the photolysis of ozone represents an effective energy dissipation process transforming solar short-wave radiation into heat, but it also codetermines the actual concentration of atomic oxygen.

Table I lists the most relevant reactions. The right column contains the temperature-dependent rate constants according to Atkinson *et al.* [1] DeMore *et al.* [2] and Hampson [3]. The system of the reaction kinetic equations, which describes the time behavior of the chemistry, consists of the equations for the five components O, O_3, H, OH, and HO_2. The most essential components are those of atomic oxygen and atomic hydrogen. This system is diurnally periodically forced by the dissociating action of solar irradiation.

In the normal case one should expect that such a system approaches a limit cycle with a period of one day. But Fichtelmann and Sonnemann [4,5], Sonnemann [6], and Sonnemann and Fichtelmann [7] found that this system is able to produce a nonlinear response. The system represents a nonlinear driven photochemical oscillator (Sonnemann and Fichtelmann [4,8]), which operates close to resonance in the vicinity of the mesopause. This oscillator can create phenomena like cascades of period doublings or chaos.

III. CONSIDERATION OF DIFFUSIVE PROCESSES IN THE CHEMISTRY OF THE MESOPAUSE

The system, investigated by Sonnemann and Fichtelmann [7], reflects atmospheric conditions only in a rather idealized way. It is a zero-dimensional model, and does not include diffusive processes. But the mesopause region is characterized by a strong increase of the turbulent diffusion. Two kinds of diffusion act in the atmosphere. These are molecular and turbulent or also eddy diffusion. Above the turbopause at about 105-km altitude the molecular diffusion begins to dominate, and leads to an increasing separation of the thermospheric constituents. Therefore this region is called the heterosphere. Below this height turbulent diffusion predominates, which results from the dissipation of various atmospheric waves particularly of the (internal) gravity waves. The turbulent diffusion results in a mixing of the atmospheric constituents in such a way that the mixing ratio of the major constituents like O_2 or N_2 is nearly constant up to the turbopause. This region is called the homosphere.

Generally, turbulence has the tendency to destroy structures. As far as that goes, it is important to know what happens if a system, which operates for example in the chaotic mode, is subjected to diffusion. In order to investigate this question a model has been established which includes the height range of nonlinear response. The consideration of the turbulent diffusion of an atmospheric RDS can be written (see, e.g., Banks and Kockarts, [9]) as

$$\frac{\partial[X]}{\partial t}=P_X-L_X[X]-\frac{\partial([X]w)}{\partial z}. \tag{1}$$

$[X]$ stands for the concentration of the species X (here $X\triangleq$ O, O_3, H, OH, and HO_2), P_X is the production term, and L_X is the loss term (linearized loss coefficient), with L_X^{-1} being the individual characteristic chemical time. z represents the height. The vertical diffusion velocity w is governed by

$$w=-K\left(\frac{1}{[X]}\frac{\partial[X]}{\partial z}+\frac{1}{H}+\frac{1}{T}\frac{\partial T}{\partial z}\right), \tag{2}$$

where K is the eddy diffusion coefficient, H the atmospheric pressure scale height, and T the temperature. Perfect mixing leads to $w=0$. Then the hydrostatic equation follows from the expression within the parentheses of Eq. (2). Such a five-component system has to be integrated using K as varying parameter. (We note that the autonomous system consists of six phase variables: the five components and time t.)

IV. MODEL DESCRIPTION

The height region of the nonlinear response amounts only to about 2 km depending on water vapor concentration, temperature, or the dissociation rates as parameters of the system. This region is located between about 79 and 86 km, and its height essentially depends on humidity. With increasing humidity the region is shifted upwards. This relatively small extension is the reason why the nonlinear response has not been discovered in atmospheric models thus far, because the

height resolution of the models is usually rougher than this extension of 2 km.

A 200 layer model has been developed with a height resolution of $\Delta z = 100$ m. The boundaries have been fixed at 92 and 72 km, sufficiently far from the region of nonlinear response. At the upper boundary atomic oxygen and atomic hydrogen, the dominating constituents, have only a weak diurnal variation, so that their concentrations have been fixed there, employing values corresponding to measurements. The other constituents show strong diurnal variations but their concentrations are only very small and determined by both the main constituents. That is the reason why they are considered to be free varying constituents. Their time-dependent concentrations have been calculated from the equations without consideration of transport. Diffusive transport is taken into calculation below this boundary layer.

At the lower boundary at 72-km altitude the conditions are different from those at the upper boundary. Here the family concentrations $[O]_{ODD}=[O]+[O_3]$ and $[H]_{ODD}=[H]+[OH]+[HO_2]$ have a reduced diurnal variation. However, the daily averaged characteristic chemical family times (for definition, see Sonnemann and Fichtelmann, [7]) are small compared with the characteristic diffusion times (Mange [10]) so that it may be justified to calculate the time-dependent lower boundary concentrations from the equations without the inclusion of diffusion. The boundary regions have been excluded (in each case 20 layers border on the boundaries) from the representation. The initial conditions influence, above all, the transient behavior, but they can also determine the asymptotic state for small diffusion coefficients. For example for a system operating in a period-2 mode it is important which phase relation two neighboring layers have. A weak diffusion is not able to synchronize different phases or, at least, a phase synchronization takes place after a very long time.

In order to provide clear conditions of consideration, some simplifications and idealizations have been introduced.

(1) The atmosphere was considered isothermal with a temperature of $T = 180$ K according to seasonal average values. Hence, the last term in Eq. (2) becomes zero, and the scale height is constant. We use an average value of $H = 6$ km. The densities of O_2 and M increase exponentially with a scale height H with decreasing height accordingly to the hydrostatic equation. The upper boundary values have been taken from the Cosmic Space Research (COSPAR) International Reference Atmosphere (CIRA 72) [11].

(2) The eddy diffusion coefficient was also considered independent of height z. Consequently, the derivative of K with respect to height in Eq. (1) also vanishes.

(3) Humidity is a sensitive parameter. Generally, the concentration amounts to few ppmv (parts per million per volume). This relatively small value corresponds to photochemical model calculations. However, observations up to 10–15 ppmv have also been published (see Grossmann *et al.* [12]. Therefore, it is widely unclear thus far how strong the water vapor-concentration can vary in this height. High thermospheric water vapor concentrations, which could be transported downward, have also been inferred from different observations by Sonnemann *et al.* [13] Frank, Sigwarth and Craven [14], and Frank and Sigwarth [15]. We choose the expression $J_{H_2O}[H_2O]/[M]$ as independent of height. This assumption may be approximately justified in this region. Since $[H_2O]/[M]$ decreases with increasing height due to the photolysis by J_{H_2O}, J_{H_2O} itself increases with height. Of course, both the effects do not absolutely compensate for each other, but we chose to ignore this here.

(4) J_{O_3} almost does not depend on height for all zenith angles less than 90° in the mesopause region. It does not decrease down to the mean mesosphere. Hence it was also considered as constant.

(5) The photolysis rate of O_2 already depends strongly on height in the mesopause. This has been taken into calculation by an exponential decrease with a scale of $2H = 12$ km for decreasing height. In other words, it decreases more weakly than O_2 rises within the model domain, so that the product $J_{O_2}[O_2]$ grows further.

(6) The forcing by radiation takes place by a step function with 12 h of overhead sun and 12 hour of night. This is a sufficiently good approximation, and it does not influence the system behavior on principle.

We used a procedure of an automatic time step control. The greatest concentration change for each time step of any constituent at any layer (both with respect to chemistry and transport) amounted partly less than 1%. During sunrise and sunset the time steps become extraordinarily small, as the calculations are extremely computer time consuming.

V. RESULTS

From a formal mathematical point of view the air density, depending on height, acts as a control parameter. $[O_2]$ is proportional to $[M]$ for a well-mixed atmosphere, and also the term $J_{O_2}[M]$ can be described as function of $[M]$ $(\sim\sqrt{[M]})$. Using a stroboscopic representation for the results of the model calculations, one obtains the well-known bifurcation diagrams. We display the density values at sunset, and show only bifurcation diagrams of the main component atomic hydrogen here. The concentrations of the individual constituents have been calculated at each layer. Hence, we prefer a geophysical representation: height via concentration. Figure 1 exhibits an example for a computer run without consideration of diffusion ($K = 0$ cm^2 s^{-1}). Generally, there is a bifurcation into period-2 oscillation if coming from below. Usually there follows a whole cascade of period doublings ending in a chaotic band. Normally the chaotic band includes varyingly broad windows of subharmonic oscillations having different periods. Frequently the chaotic band finishes at the upper border by a catastrophic bifurcation into a period-3 oscillation, and that region ends by a catastrophic bifurcation, again jumping into the fundamental mode. Above the second chaotic band appear a period-4, -3, and -5 windows in succession. The height resolution is, however, too coarse to display the transition between the different windows clearly. The picture of occurrence can vary strongly if one uses different parameter sets for the calculation (such as rate constants, temperature, photolysisrates, etc.).

Now we consider what will happen if the eddy diffusion coefficient comes from high values, and reduce it step by step. Figures 2(a)–2(f) show computations for a humidity of 4 ppmv. Each run begins with the same initial conditions. As

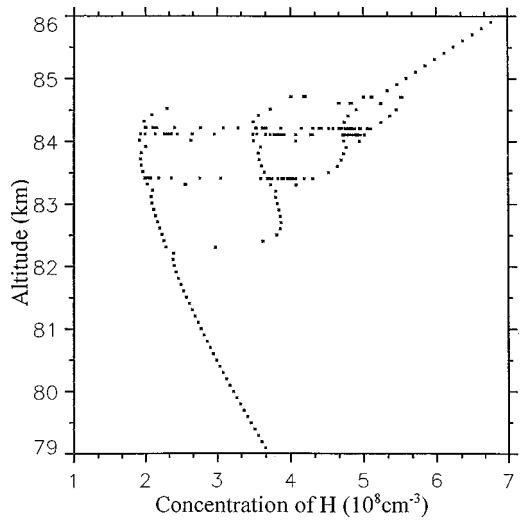

FIG. 1. Bifurcation diagram for the atomic hydrogen concentration without consideration of diffusion for a water vapor concentration of 4 ppmv. Coming from below, the diagram starts with a subtle bifurcation into a period-2 window. The figure shows the sunset values in a stroboscopic representation.

supposed the system operates in the fundamental mode [Fig. 2(a)] for high diffusion coefficients ($K > 1.2\times10^5\,\mathrm{cm^2\,s^{-1}}$). The system nearly approaches a limit cycle after several days. A first subtle bifurcation into a weak period 2 seems to take place for $K \lesssim 1.2\times10^5\,\mathrm{cm^2\,s^{-1}}$. We will show later that the system operates in a metastable state in the vicinity of this value. It is not clear thus far how strong this faint period-2 oscillation is influenced by the numerical procedure. Figure 2(b) shows a long ranging sickle-shaped region of the apparent occurrence of a period-2 window. The amplitude difference suddenly increases strongly for a certain value of K, and simultaneously the height extension of the period-2 window commences to shrink, so that the period-2 window disappears again in constant heights on the edges of the region of period-2 oscillation. The whole diagram assumes a sickle-shaped (for other parameters more an onion-shaped) appearance [Fig. 2(b)]. Reducing K further, there occur period doublings in succession in the upper part of the diagram [Fig. 2(c)], which finally exceeds into chaotic behavior [Fig. 2(d)]; note that the concentration scale has been changed. For this example the chaos surprisingly passes into a behavior marked by the occurrence of exclusively subharmonics. In the upper part of the diagram a broad period-6 oscillation occurs, and in the lower part a period-2 [Fig. 2(e)] window appears.

The appearance of the diagrams always differ from those bifurcation diagrams of the Feigenbaum route—the so-called pitchfork diagrams. There the bifurcations takes place under an angle of 180° at the point of bifurcation; here the angles are either zero or, at least, almost zero like an onion spire. That is why this behavior has been called onion bifurcation.

Using the diffusion coefficient in a direct way as a control parameter, and considering the response in constant heights, we can show the bifurcation behavior more clearly. In the computer run we have reduced the diffusion coefficient step by step by a quotient of 1.2 using the old final values as new initial values. For each step 25 days were computed, and the first 12 days were deleted. We consider the bifurcation behaviors in 85.5, 85, 84.5, 84 and 83 km, respectively. The parameters are the same as those used in the graphs of Fig. 2. In order also to show the behavior for small diffusion coefficients with sufficient resolution, we use a logarithmic scale for K. Figures 3(a)–3(e) exhibit the results. Figure 3(a) displays the bifurcation diagram at the uppermost height. The picture illustrates the finding mentioned above. The period doubling disappears for strong and weak diffusion, for weak diffusion due to the shrinking of the height region of nonlinear response. In general, the figures show that different critical thresholds of the diffusion coefficient occur for which the qualitative behavior of the attractor changes.

At 85 km [Fig. 3(b)], the system runs into a chaotic band for small values of K. This chaotic band is obviously marked by an internal structure. Maybe there are periodic windows within the chaotic band, but it is impossible to find them out on the basis of this coarse procedure. The computation of periodic windows within a chaotic band normally starts with long lasting transient chaos, and approaches the periodic attractor only after many orbits. That means there is no guarantee that the transients have sufficiently died away after 13 days. Therefore, an investigation of the fine structure of chaos requires a special treatment. In other cases, also after subtle bifurcations, as the computations show, the old final values are sufficiently close to the new final values after a small step of the control parameter. Hence the convergence is very fast. In contrast to this, all catastrophic bifurcations are marked by long lasting transients. Thus it is also necessary in this case to calculate essentially more orbits around the catashophic bifurcation point.

Coming from high diffusion coefficient values, all of Fig. 3. show a bifurcation into a period-2 window. As stated earlier, there seems to be a very weak subtle bifurcation, and after that a strong jump into a period-2 window marked by large amplitude differences. The manner of transition is not clear in these figures. Figure 4(a) exhibits a refined resolution around this spot. Starting with $K = 1.2\times10^5\,\mathrm{cm^2\,s^{-1}}$ and reducing the diffusion coefficient by a quotient 1.015 after each 25 days, the bifurcation diagram shows a jump between $K = 1.1306\times10^5$ and $1.1119\ \mathrm{cm^2\,s^{-1}}$ [in a logarithmic scale between 11.636 and 11.621, as seen in Fig. 4(a)]. The sixth step from the right seems to represent the transition. Apparently these values already belong to the strong oscillating period-2 window but 25 days were not long enough to approach a new attractor. This is shown in Fig. 4(b). We start our computation with $K = 1.113\times10^5\,\mathrm{cm^2\,s^{-1}}$. After a transient period of approximately 20 days marked by an overswing of the H concentration, the system seems to approach a limit cycle of period 2 with a constant or, at least, very weak oscillating amplitude. Obviously this limit cycle is unstable. The amplitudes begin to amplify and the system runs into a limit cycle of period 2 marked by a large amplitude difference. This transition time sensitively depends on small initial perturbations. The computer precision influences the transition time but not the final state. Figure 5 shows the system response to a perturbation near but above the critical turbulence ($K = 1.2\times10^5\,\mathrm{cm^2\,s^{-1}}$). After 100 days the atomic hydrogen concentration was multiplied by a factor 1.1. The system responded with an attenuating period-2 os-

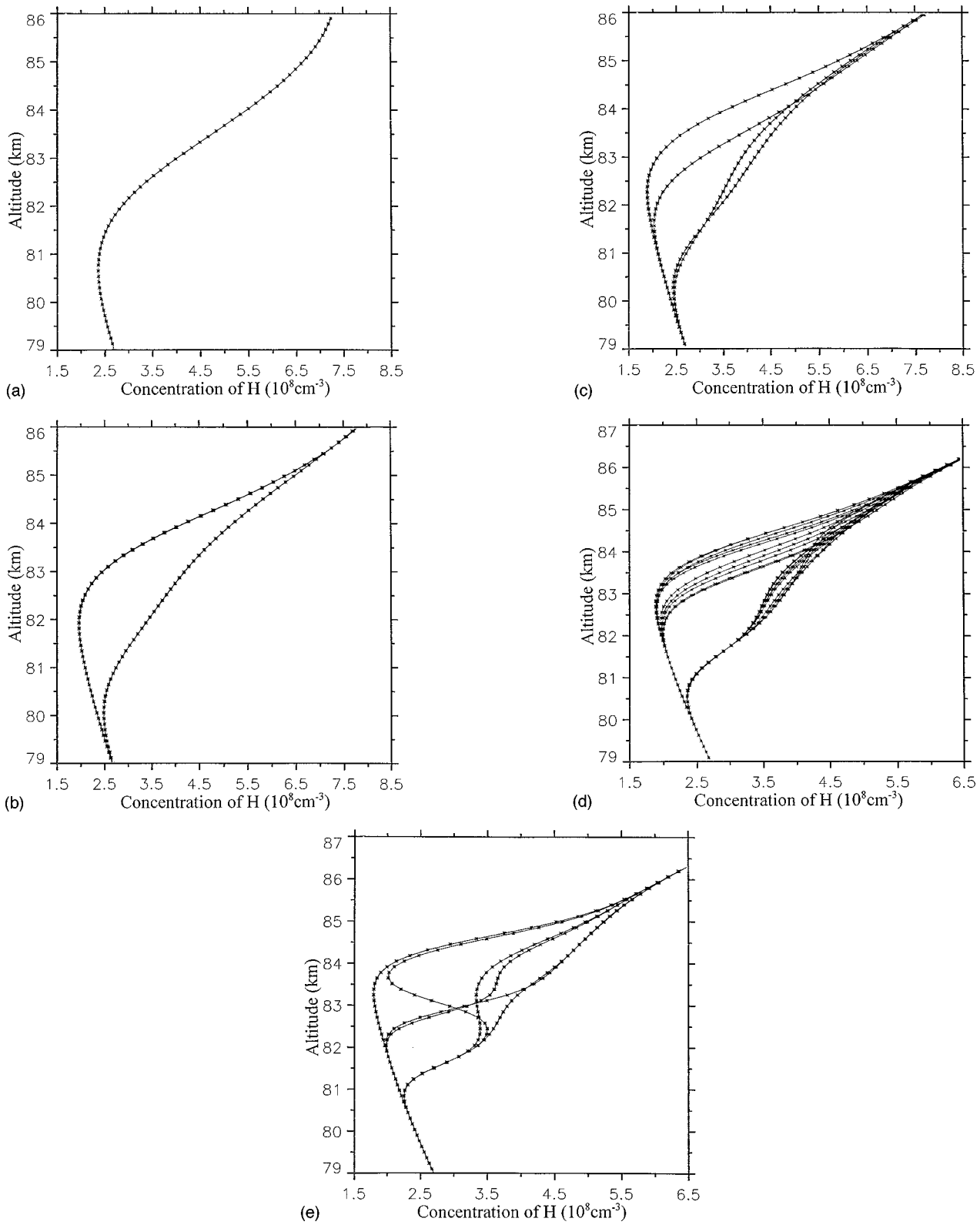

FIG. 2. Bifurcation diagrams for varying diffusion coefficients K [$K=1.2\times10^5$; 9×10^4; 4×10^4; 2×10^4; and 7×10^3 cm^2 s^{-1} for (a), (b), (c), (d), and (e), respectively]. The same parameters as in Fig. 1 are used. The figures illustrate the onion bifurcation.

cillation approaching that state again which turned up before the perturbation. The calculation gives evidence for a catastrophic bifurcation into a period-2 window marked by a high amplitude difference of two succeeding days for a critical turbulence parameter.

VI. DISCUSSION AND CONCLUSIONS

The computations show that reaction-diffusion systems, which are able to respond nonlinearly, can create a large number of different bifurcations. Although there occur phe-

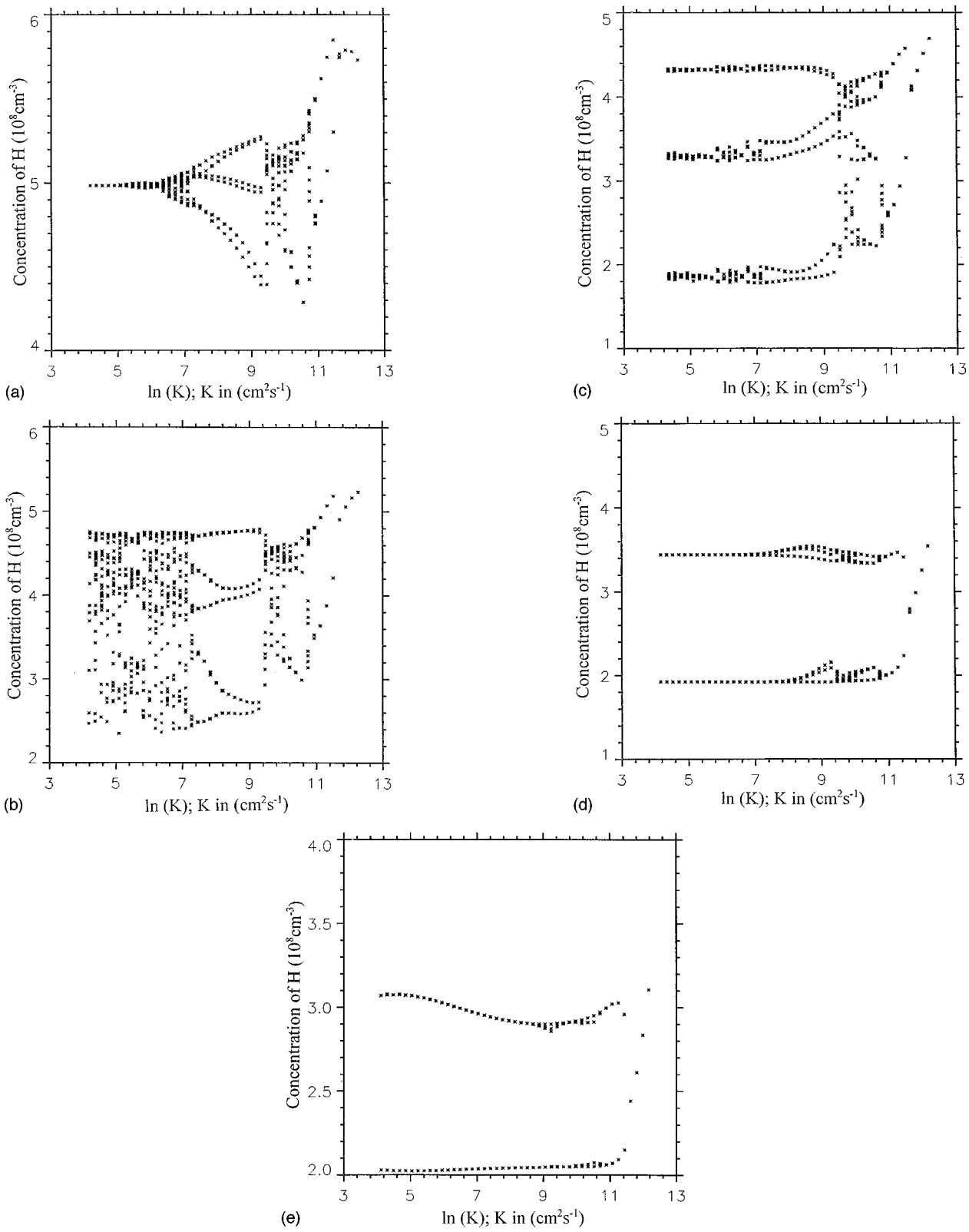

FIG. 3. The diffusion coefficient K is used as control parameter and the bifurcation behavior was considered at constant heights z [$z = 85.5$, 85, 84.5, 84, and 83 km for (a), (b), (c), (d), and (e) respectively]. The diffusion coefficient was reduced every 25 days by a quotient of 1.2 using the old final values as new initial values. The same parameters as in Fig. 1 are used. There are various catastrophic bifurcations. A logarithmic scale was employed for K.

nomena like cascades of period doubling, periodic windows, and chaos, the appearance of these effects differ from those to be seen in the discrete logistic map or in nonlinear systems of ordinary differential equations. This is valid for the so-called onion bifurcation or for the catastrophic bifurcation from the ground mode, or perhaps one faint period-2 oscillation into a strong period-2 oscillation.

Considering the atmosphere, the turbulent diffusion coef-

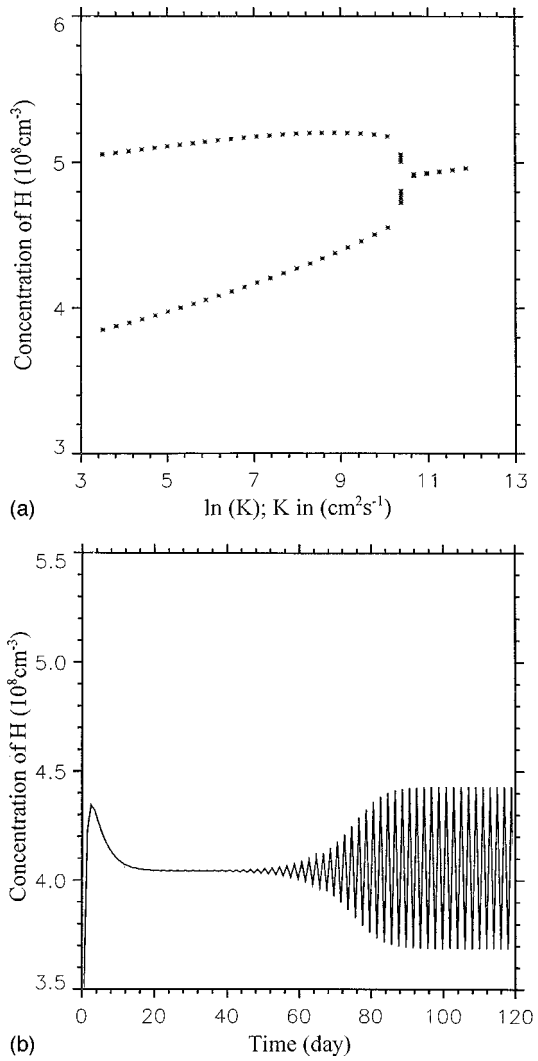

FIG. 4. (a) Higher resolution around the spot of catastrophic bifurcation in a period-2 window at a height of 85 km. K is on a logarithmic scale, and the same parameters are used as in Fig. 1. The diffusion coefficient was reduced every 25 days by a quotient of 1.015. (b) Behavior of the transition from a metastable state into a stable period-2 oscillation for a diffusion coefficient of $1.113 \times 10^5\,\mathrm{cm^2\,s^{-1}}$ at a height of 85 km. This time of transition depends sensitively on the accuracy of the program and on the computer precision. In contrast to this, the final state does not depend sensitively on the computer precision. The same parameters are used as in Fig. 1.

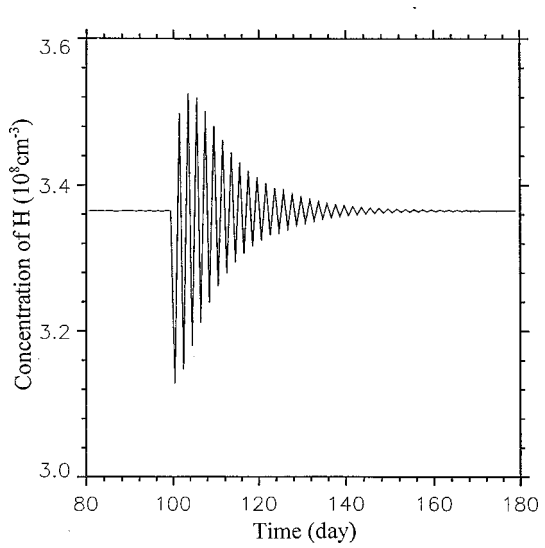

FIG. 5. System response to a perturbation near the critical turbulence for a diffusion coefficient of $1.2 \times 10^5\,\mathrm{cm^2\,s^{-1}}$. The same parameters are used as in Fig. 1.

ficient amounts to the order of $n \times 10^5\,\mathrm{cm^2\,s^{-1}}$ in about 80–85-km height. There is a large scatter (see, e.g., Hocking [16]) of one order in magnitude exceeding values of $10^6\,\mathrm{cm^2\,s^{-1}}$ and perhaps dropping below $10^5\,\mathrm{cm^2\,s^{-1}}$. Lübken [17] published measurements of mean profiles of the turbulent diffusion coefficient which show values as low as $10^4\,\mathrm{cm^2\,s^{-1}}$ in the region of nonlinear response in summer. But there is also a great lack of measurements of the diffusion coefficient, and a large degree of uncertainty.

A real nonlinear behavior of the photochemistry within the mesopause region is most probably possible only under quiet conditions, which means under low gravity wave activity. It is unlikely that higher subharmonics or chaos, which result from the photochemistry and are not imprinted by external forces like the dynamics can appear. The only remaining possibility seems to be that a period-2 oscillation can occur. Other effects are suppressed by the strong atmospheric diffusion for these examples. But we have to emphasize that our result only reflects very special conditions, and does not encompass the whole atmospheric variability. This concerns the idealizations of the model, the boundary conditions, the duration of daytime hours (reflecting season), the water vapor concentration, etc.

There are numerous indications of a period-2 oscillation, namely, the so-called quasi-two-day wave in the upper mesosphere-and lower thermosphere (sometimes observed down to the stratosphere). Such two-day waves have been found in the prevailing wind (Müller [18], Clark [19], Poole [20], Jacobi, Schminder, and Kürschner [21], and further), in temperature (Wu *et al.* [22]), or in the oxygen green line volume emission rate (Ward, Solheim, and Shepherd [23]). The phenomena were interpreted in terms of dynamical causes and, indeed, the thermic forcing by a two-day chemical heating is too small to explain the observed temperature variations.

However, dynamics and chemistry are closely fed back. It cannot be excluded that there is an amplification effect. The model under consideration does not take into calculation the advective transport, but vertical winds convey chemically active species from the thermosphere into the mesopause region. This advective transport can be stronger than the diffusive transport. In order to decide the question of whether there is a real chemically induced two-day wave or not, one needs interactive operating global three-dimensional models of the dynamic and chemistry which are not available thus far.

That there is only a quasi-two-day period and not exactly a two-day period could easily be explained by the zonal movement of the air. An air parcel moves with or against the rotation of the Earth; that means its effective period of solar illumination is less or greater than one day. Consequently, a subharmonic period-2 window is also less or greater than

two days. We have called this the photochemical Doppler effect. Taking into calculation the real zonal velocities amounting to some 10 ms^{-1}, the periods differ from one day up to few hours, as found for the quasi-two-day waves.

It may seem that such an investigation is only confined to this special atmospheric problem because a control parameter, the air density, varies simultaneously with height, meaning from layer to layer. However, it is also imaginable that other (control) parameters could vary with height or with a different space coordinate, for example temperature or a concentration having a certain gradient. Diffusion plays an important part in many natural processes. On the cellular level, for instance, the weak molecular diffusion acts, and various nonlinear reactions take place. The purpose of this paper also consists in the intention to focus the readers attention onto nonlinear reaction-diffusion systems.

[1] R. Atkinson, D. L. Baulch, R. A. Cox, Jr., R. F. Hampson, J. A. Kerr, and J. Troe, Atmos. Environ., Part A **26A**, 1187 (1992).
[2] W. B. DeMore, S. P. Sander, D. M. Golden, M. J. Molina, R. F. Hampson, M. F. Kurylo, C. J. Howard, and A. R. Ravishankara, Jet Propulsion Laboratory Report No. 90-1, NASA Panel for Data Evaluation, 1990.
[3] R. F. Hampson, U.S. Department of Transportation Report No. FAA-EE-80-17, 1980.
[4] B. Fichtelmann and G. Sonnemann, Acta Geod. Geophys. Mont. Hung. **22**, 313 (1987).
[5] B. Fichtelmann and G. Sonnemann, Ann. Geophys. (Eur. Geophys. Soc.) **10**, 719 (1992).
[6] G. Sonnemann, *Ozone—Its Natural Variability and Anthropogenic Influence* (Akademie Verlag GmbH, Berlin, 1991), pp. 263–282 (in German).
[7] G. Sonnemann and B. Fichtelmann, J. Geophys. Res. **102**, 1193 (1997).
[8] G. Sonnemann and B. Fichtelmann, Acta Geod. Geophys. Mont. Hung. **22**, 301 (1987).
[9] P. M. Banks and G. Kockarts, *Aeronomy* (Academic, New York, 1973), Pt. B.
[10] P. Mange, J. Geophys. Res. **62**, 279 (1957).
[11] *CIRA 72, COSPAR International Reference Atmosphere 1972*, edited by A. C. Stickland (Akademie-Verlag, Berlin 1972).
[12] K. U. Grossmann, W. G. Frings, D. Offermann, L. André, E. Kopp, and D. Krankowsky, J. Atmos. Terr. Phys. **47**, 291 (1985).
[13] G. Sonnemann, D. Felske, R. Knuth, L. Martini, and B. Stark, Space Res. **XVII**, 265 (1977).
[14] L. A. Frank, J. B. Sigwarth, and J. D. Craven, Geophys. Res. Lett. **13**, 307 (1986).
[15] L. B. Frank and J. B. Sigwarth, Rev. Geophys. **31**, 1 (1993).
[16] W. K. Hocking, Adv. Space Res. **10**, 153 (1990).
[17] F.-J. Lübcken, J. Geophys. Res. **102**, 13 441 (1997).
[18] H. G. Müller, Philos. Trans. R. Soc. London, Ser. A **271**, 585 (1972).
[19] R. R. Clark, J. Atmos. Terr. Phys. **51**, 617 (1989).
[20] L. M. Poole, J. Atmos. Terr. Phys. **52**, 259 (1990).
[21] Ch. Jacobi, R. Schminder, and D. Kürschner, J. Atmos. Terr. Phys. **59**, 1277 (1996).
[22] D. L. Wu, E. F. Fishbein, W. G. Read, and J. W. Waters, J. Atmos. Sci. **53**, 728 (1995).
[23] W. E. Ward, B. H. Solheim, and G. G. Shepherd, Geophys. Res. Lett. **24**, 1127 (1997).